3D-Printed Airfoil Wind Tunnel Aerodynamic Testing and Simulation

Rapee Ujjin*, Choosak Ngaongam, Sudarat Chaikaindee and Pornthep Boonyanetra

Department of Aviation Maintenance Engineering, College of Engineering, Rangsit University, Pathumthani, Thailand
*Corresponding author, E-mail: rapee.u@rsu.ac.th

Abstract

In this paper, the experimental testing of NACA 2415 airfoil in the wind tunnel has been performed to obtain aerodynamic characteristics, which are the coefficient of lift (C_L) and coefficient of drag (C_D). The 3D printing process of fused deposition modeling (FDM) has been used to manufacture testing specimens. The wind tunnel testing models included a printed model, printed model coated with acrylic paint, and polished surface finishing model. The computational fluid dynamics (CFD) of NACA 2415 airfoil model has been constructed to study the lift and drag characteristic. CFD model simulates flow at the air velocities of 10, 15, 20, and 27 m/s and at the angle of attack of 15°, 0°, 10°, and 15°. It has been found that the lift coefficients from all tested models were agreed with simulation results and NACA 2415 airfoil data. Drag coefficient yielded close relation among tested models but inconclusive when comparing to simulation result below 10°. Both average C_L and C_D from surface finishing model can be increased up to 12% and 27% respectively at Reynolds number of $2.2x10^5$. Smoother surface finishing is capable of drag reduction and also lift production. Certain roughness degree on the airfoil surface can help to delay flow separation; therefore, surface finishing of airfoil affects airfoil characteristic, which can increase aerodynamic efficiency.

Keywords**:** *Fused deposition modeling (FDM), Computational fluid dynamics (CFD), Co-efficient of lift (C_L), Co-efficient of drag (C_D)*

1. Introduction

Wind tunnel testing is a typical experiment to determine an aerodynamic performance of the object. The testing specimen can be manufactured from several suitable materials and different methods such as a handcrafted wooden sample, molded thermosetting plastic, foam core with coated fiberglass, and so on. 3D printing technology is now capable of producing high strength with high quality of the product as comparing to traditional method as known as computer numerically control (CNC) cutting method. Three most popular printing technologies include Stereolithography Apparatus (SLA), Selective Laser Sintering (SLS), and Fused Deposition Modeling (FDM). 3D printing is one of the product manufacturing methods used when high accuracy is needed such as prototype, jig, and fixture. Many different materials can be used in 3D printing depending on the user's considering factors such as cost, time, accuracy, strength, and specific purposes. The most advantageous of this technology is reproductive of the product. FDM is considered to be a cost-effective and fast method for prototyping a new product. Repetition of specimen fabrication is usually required for experimental testing for consistency. Nevertheless, the important disadvantages of FDM is that surface roughness of printed part is excessively rough compared to other 3D printing processes (Alsoufi & Elsayed, 2017; Krolczyk, Raos, & Legutko, 2014).

Fused deposition modeling (FDM) is an additive manufacturing method that builds parts layer by layer by heating the material filament to a semi-liquid state through the print head. The softened material filament is then extruded in x and y coordinates before moved on next upper layer of z-direction by a numerical control mechanism from computer aid manufacturing (CAM).

Olasek and Wiklak (2014) evaluated 3D printing techniques specifically for aerodynamic study, which were Multi-Jet Modeling (MJM), Selective Laser Sintering (SLS), and Fused Deposition Modeling (FDM). They applied these 3D printing techniques to fabricate NACA 0018 airfoil samples for analysis, which included surface roughness, strength, detail quality, surface imperfections, and irregularities. It had been found that each printout had different surface roughness level, but overall qualities were adequate for aerodynamic testing.

NACA airfoils have appeared in many aerodynamic studies since their advantageous is adaptable to a variety of aerodynamic object design. Parashar (2015) was also interested in working on the calculation of aerodynamic characteristics, which included NACA 23012, 23015 and 2415 by using CFD code FLUENT. His study was applied to a 2-dimensional airfoil with the angle of attack from -15 to 15º at one constant velocity value. The aerodynamics characteristics, coefficient of lift and drag, had a fair agreement to the theory from Abbott and Doenhoff (1959). Kumar, Tomar, Kumar, and Jain (2015) developed a MATLAB code for NACA 2415 at a low Reynolds number with varying angle of attack from 0 to 12º. They stated that the results were found to be in good agreement with the theory. While Sogukpinar and Bozkurt (2015) used SST Turbulent model to simulate NACA 2415 at single Reynolds number, their CFD results were compared with wind tunnel experimental results, showing good agreement at a low angle of attack but not good at a high angle of attack. They claimed that it might be due to the imperfection around the airfoil section.

Srivastava, Tiwari, and Singh (2017) had used ANSYS FLUENT to simulate NACA 2415 airfoil at different low Reynolds numbers and angles of attack. They concluded that pressure and velocity were greatly influenced by a Reynolds number and an angle of attack. Aerodynamic performance from 2-dimensional analysis such as the coefficient of pressure and the coefficient of lift could be calculated with corresponding Reynolds number. Jain, Jain, and Bajpai (2016) had constructed a 3-dimensional wing model from NACA 2415 airfoil with a modification of the root profile and an addition of a dihedral angle of 6º. The simulation had performed using ANSYS FLUENT CFD software at low Renolds number to obtain airfoil characteristics successfully.

Velázques, Nožička, and Vavřín (2010) performed experimental testing in wind tunnel to measure aerodynamic characteristics of 2-dimensional of modified NACA 2415 airfoil. The airfoil models were made of expanded polystyrene foam (EPS) and coated with a layer of solid polystyrene. Velázques and Nožička (2013); Velázques and Nožička (2014) went on their study by performing computational simulation and analysis on a 2-dimensional airfoil using CFD ANSYS FLUENT to verify aerodynamic characteristics of NACA 2415 airfoil with extension to another 4 airfoil modifications. Lift, drag and moment coefficients at different angles of attack were able to obtain directly from the CFD software. Ghods (2001) had achieved wind tunnel testing on NACA 2415 to find the aerodynamic performance and found that the coefficient of lift agreed with airfoil data except the excessive drag encountered from the airfoil model. The problem was from the construction process. The model had made from resonated fiberglass on foam core with plastic paint that contained irregularities and concavities on the surface.

Krolczyk, Raos, and Legutko (2014) had investigated surface roughness and texture of parts using turning and fused deposition modeled manufacturing using an Infinite Focus Measurement Machine (IFM). They found that surface integrity FDM parts could be measured their value of roughness parameter (R_k), which had higher surface roughness than other ordinary surface finishing method. Alsoufi and Elsayed (2017) had examined surface roughness of 3D printed parts from advanced polylactic acid material (PLA+) by using FDM process with different parameters, nozzle diameter, layer height, nozzle temperature, print speed, and infill density. According to their results, in terms of part quality finish, the optimal parameter was using 0.3 mm of nozzle diameter and 0.1 mm of layer height, which achieved an average surface roughness value (R_a) of 1.29 μm due to smallest layer height printing capability of the printer.

Harun, Abbas, Dheyaa, and Ghazali (2016) had performed aerodynamic testing of NACA 0026 airfoil in wind tunnel with a highly-ordered rough surface, silicone rubber riblets surface strip, attached near the leading edge of the specimens. Testing airfoils were been manufactured from wood and aluminum. They found that attaching a uniformed pattern arrangement surface riblets at the specified area over airfoil could cause thicken in the boundary layer, which results in skin friction reduction up to 25%. Unlike other shapes such as circular cylinder, Rodríguez et al. (2016) had found in their experimental results that an increase in surface roughness (k_s = 0.02D) around circular cylinder object would instantly increase skin friction drag because of an early of separation of the boundary layer. Drag coefficient increased from 0.3 up to 1.122 at Re = $4.2x10^5$.

White et al. (2011) have tested NACA 63_3-418 airfoil with a sandblasted surface treatment to investigate airfoil performance. They found that by increasing the level of roughness at the leading edge area to 70 μm could cause decreasing in maximum lift coefficient and increasing profile drag coefficient.

Zhou and Wang (2012) had studied surface roughness on SD7003 airfoil by placing roughness bump near the leading edge of the wing in order to increase aerodynamic performance. Roughness bump was a large scale of irregular surface waviness, which delayed flow separation. The result showed that the friction drag was increased but with a significant reduction of pressure drag and slightly increasing of lift. The overall lift to drag ratio was increased. Abdel-Rahman and Chakroun (1997) had conducted an experiment in wind tunnel of a NACA 0012 airfoil with different roughness of p80 and p120 sandpaper roughness surface. They concluded that the drag coefficient increased with an increasing roughness size and caused a reduction in lift up to 10° angle of attack. Beyond 10° angle of attack, lift tended to increase because of roughness is found to delay the separation.

2. Objectives

1. To improve specimen manufacturing quality from FDM for aerodynamic testing in a wind tunnel.
2. To construct a CFD model and perform simulation of NACA 2415 airfoil in order to obtain aerodynamic forces prediction.
3. To study the effects of different surface roughness on aerodynamic efficiency.
4. To compare the aerodynamic characteristics of different surface roughness finishing airfoils with the simulation results from the CFD model.

3. Aerodynamic Characteristics

3.1 Aerodynamic lift and drag from an airfoil

Aerodynamic lift from an airfoil is a reaction force that has been exerted from the differential pressure that acts between the upper and lower airfoil surface area. The differential in pressure depends on the shape, thickness and lifting ability of the airfoil. Lifting ability is known as lift coefficient, which will vary with angle of attack (Anderson, 2012). The amount of lift obtained from the airfoil is proportional to the dynamic pressure from air velocity and wing area. The lift force can be described by the following formula:

$$L = C_L \frac{1}{2} \rho v^2 A$$

Where: L = lift force (N),
C_L = lift coefficient (-),
ρ = density (kg/m^3),
v = velocity (m/s),
A = area (m^2)

Aerodynamic drag from an airfoil is a force induced by relative air velocity that proportional to the dynamic pressure of the air and the area on which it acts. Drag varies with the shape of the body, surface roughness, and other factors; therefore, the drag coefficient is used to describe how much of the dynamic pressure force gets converted into drag (Anderson, 2012). The general formula for drag force is:

$$D = C_D \frac{1}{2} \rho v^2 A$$

Where: D = drag force (N),
C_D = drag coefficient (-),
ρ = density (kg/m^3),
v = velocity (m/s),
A = area (m^2)

3.2 Reynolds number

A Reynolds number is used to measure the viscous qualities of fluid. At low Reynolds numbers, the flow is laminar while at high Reynolds numbers; it is considered turbulent. Therefore, higher velocities or longer distance downstream of the airfoil tend to produce higher Reynolds numbers and consequently greater potential for turbulent flow (Smith, 1992). It is customary to use a characteristic length to define Reynolds number, which normally refers to average wing chord or chord length of a rectangular wing planform in this paper. Reynolds number is defined as follows:

$$\mathrm{Re} = \frac{\rho \mathrm{vx}}{\mu}$$

Where: Re = Reynolds number (-),
ρ = density (kg/m^3),
v = velocity (m/s),
x = average chord length (m),
μ = air viscosity (kg/m·s)

3.3 Lift slope

Lift slope is the change in lift coefficient with respect to the angle of attack, which is normally expressed in a unit of lift coefficient per degree. An infinite lift slope (a_0) can be found from standard airfoil data signifying 2-dimensional airfoil. Once a cross-sectional of the airfoil has been extended spanwise to present a wingspan, lift slope will be changed due to the presence of downwash, which results in a decrease in lift slope. The finite lift slope (a), 3-dimensional airfoil slope, can be determined by knowing span efficiency factor (e) and wing aspect ratio (AR). The corresponding lift slope equations are as follows:

$$a_0 = \frac{dC_L}{d\alpha}$$

$$a = \frac{a_0}{1 + 57.3a_0 / (\pi e \mathrm{AR})}$$

Where: a_0 = infinite lift slope (-),
C_L = lift coefficient (-),
α = angle of attack (^{o}),
a = finite lift slope (-),
e = span efficiency factor (-),
AR = wing aspect ratio (-)

4. Materials and Methods

4.1 CFD modeling

A NACA 2415 airfoil model was constructed in SolidWorks simulation software. NACA 2415 airfoil geometries were taken from airfoil data (Abbott & Doenhoff, 1959; Selig, Lyon, Giguere, Ninham, & Guglielmo 1996). Airfoil chord length and span were 0.10 and 0.12 m respectively. The simulation was performed with no roughness defined on both upper and lower surfaces of the airfoil. Figure 1 shows the geometry of the NACA 2415 airfoil (a) and 3-dimensional airfoil model in the simulation (b). The model was simulated at different air velocities and angles of attack at mean sea level conditions. Table 2 shows boundary conditions and values for the simulation.

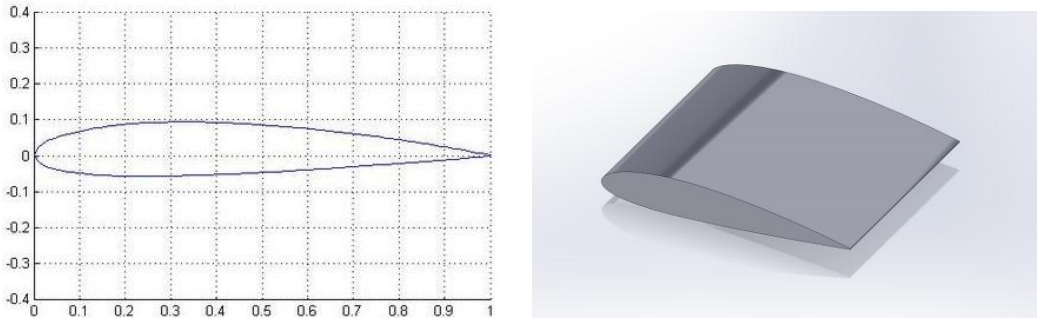

(a) (b)

Figure 1 NACA 2415 airfoil (a) Geometry (b) 3D model

Table 1 Boundary conditions and values for 3D simulation

Boundary	Value	Unit
Altitude	Mean sea level	m
Air density (ρ)	1.225	kg/m^3
Air pressure (p)	$1.01325x10^5$	N/m^2
Air viscosity (μ)	$1.7894x10^{-5}$	kg/m·s
Air temperature (T)	288.16	K
Angle of attack (α)	-15, 0, 10, 15	Degree (º)
Fluid flow velocity (v)	10, 15, 20, 27	m/s

4.2 Specimen preparation

Since fused deposition modeling (FDM) was less time consuming, uncomplicated and cost-effective for the reproduction of sample, the FDM printing was then used for manufacturing NACA 2415 airfoil for wind tunnel testing. Alunar M508 3D desktop printer was used to fabricate specimen as shown in figure 2. Full-scale model in simulation has also been used in printing model. There were 3 specimens to be tested in a wind tunnel with different surface roughness. Once all 3 the specimens were printed, two of them were primed with surface primer and sanded to remove all surface irregularities and then applied 3 coated of acrylic paint for smoother surface finishing. One out of painted specimens was further treated with the polishing process for a smoother surface. Prior to testing, the surface roughness of printed, painted, and polished specimens were validated using a direct comparison with standard roughness specimen scale to indicate surface roughness values, which were determined to be 10, 5, and 2 μm respectively. Printed quality from Alunar M508 3D desktop printer was capable of 10 μm, which was achieved by choosing a minimum layer height of 0.1 mm. The printing process parameters of the operating setup are shown in table 2.

Table 2 Summary of the operating **setup** of FDM 3D printer

Parameters	Values
Filament Material	PLA
Color	White
Process	FDM
Layer Height (mm)	0.1
Nozzle Diameter (mm)	0.3
Infill Density (%)	20
Nozzle Temperature (°)	200
Printing Speed (mm/s)	30
Cooling Fan Rate (%)	50
Bed Temperature (°)	50
Room Temperature (°)	25

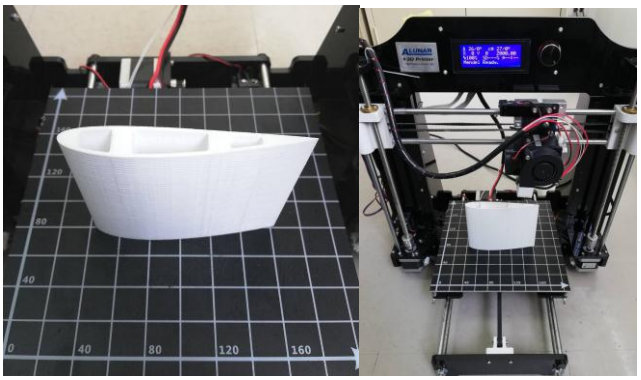

Figure 2 Printed NACA 2415 airfoil on FDM printer

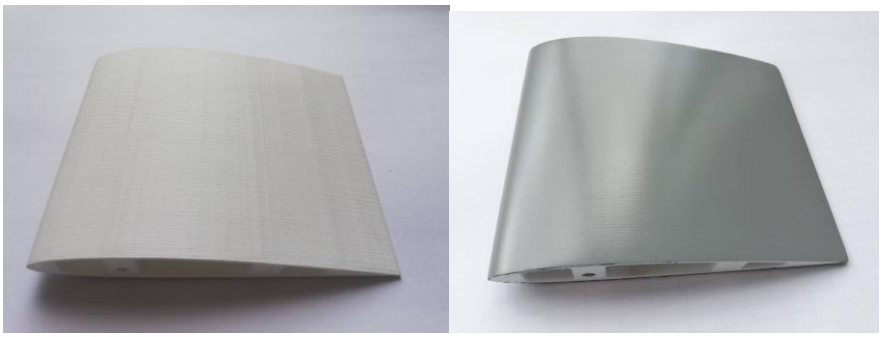

(a) (b)

Figure 3 Printed NACA 2415 with (a) No surface finishing and (b) Acrylic painted surface finishing

4.3 Wind tunnel experimental testing

The experimental testing had been conducted at the low-speed open circuit wind tunnel, Gunt HM170, in Fluid Mechanic Laboratory, College of Engineering, Rangsit University. The test section of the wind tunnel was 0.3 m wide, 0.3 m high, and 0.4 m long. HM 170.60 data acquisition system had been used for lift and drag force collection. All three specimens, printed, painted and polished specimen were tested at velocities of 10, 15, 20, and 27 m/s and angles of attack of -15, 0, 10, and 15° in testing conditions as shown in Table 3. The results from wind tunnel testing will then be compared to simulation results.

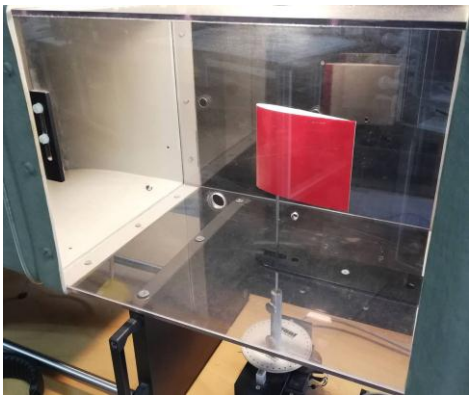

Figure 4 Wind tunnel experimental setup

Table 3 Wind tunnel experimental testing conditions

Boundary	Value	Unit
Air density (ρ)	1.225	kg/m^3
Room temperature (T)	29.7	(ºC)
Angle of attack (α)	-15, 0, 10, 15	Degree (º)
Fluid flow velocity (v)	10, 15, 20, 27	m/s

5. Results and Discussion

The results from wind tunnel testing were quantitative since all of 3 specimens had been tested at 5 different air velocities and 4 different angles of attack. It had been found from figure 5 that lift force were grouped within the same air velocity. Among 3 tested airfoils, printed airfoil yielded the highest lift for all velocity range, and the least producing lift was painted airfoil. Velocity grouping was also in drag value but not really distinctive as lift value. However, printed and polished airfoil had almost the same amount of drag but higher than painted airfoil, which was shown in figure 6. It was noticeable that all airfoils had the same zero lift angle, which was approximately 2°.

The lift and drag coefficient were all averaged for each angle of attack. Each average value of coefficient represented the coefficient of lift and drag at the particular angle of attack. In terms of lift coefficient, all of the tested airfoil coefficients and simulation results were agreed with NACA 2415 airfoil data, which were shown in figure 7 (a). Finite lift slope had been calculated by assuming span efficiency factor (*e*) of 0.85 as a typical rectangular wing planform in subsonic flow. Due to the size and effective testing area in the wind tunnel, low aspect ratio airfoil value of 0.83 was allowed in the testing. Printed, painted and polished specimens yielded value of 0.0213, 0.0222, and 0.0225 of finite lift slope respectively. Finite lift slope from the simulation was determined to be 0.0266, while NACA 2415 airfoil data was 0.0249, as shown in table 4. The polished specimen had the highest finite lift slope among all 3 specimens, which meant it had better lift increasing rate per degree and had 9.4 % difference when comparing to NACA 2415 airfoil data lift slope, while the simulation result had only 7.0 % difference.

For the coefficient of drag value, polished airfoil seemed to have a little higher value than printed and painted airfoils at a positive angle of attack. There was no relation of the drag coefficient between wind tunnel and simulation results, which results in an increase in L/D ratio of the simulated model across the tested angle of attack range. The simulation tended to have a very low coefficient of drag because there was an ideal frictionless flow condition.

Between 10° to 15°, it had been noted that printed and painted airfoils, which had different surface roughness but gave relatively the same L/D ratio. However, below 10°, both surface-finished airfoils had almost the same L/D ratio. Figure 8 showed that the printed airfoil without surface finishing, which had the highest roughness surface, produced the highest drag among the other airfoils but yielded the highest lift; therefore, was the best L/D ratio airfoil for all angle of attack range.

When comparing between painted and polished airfoil between 0° to 15°, the lift had increased up to 15% and so as the drag which increased up to 20% at the maximum tested Reynolds Number of $2.2x10^5$; thus, consequent in a reduction of L/D ratio. At 10°, painted and polished airfoil had an average coefficient of lift of 0.2555 and 0.2813, and the coefficient of drag of 0.0731 and 0.0836 respectively; therefore, yielded an increase in C_L and C_D, 10% and 14.3%. However, at 15°, an increase in C_L and C_D became 12% and 27% from the average coefficient of lift of 0.400 and 0.4486, and coefficient of drag of 0.1123 and 0.1426 respectively.

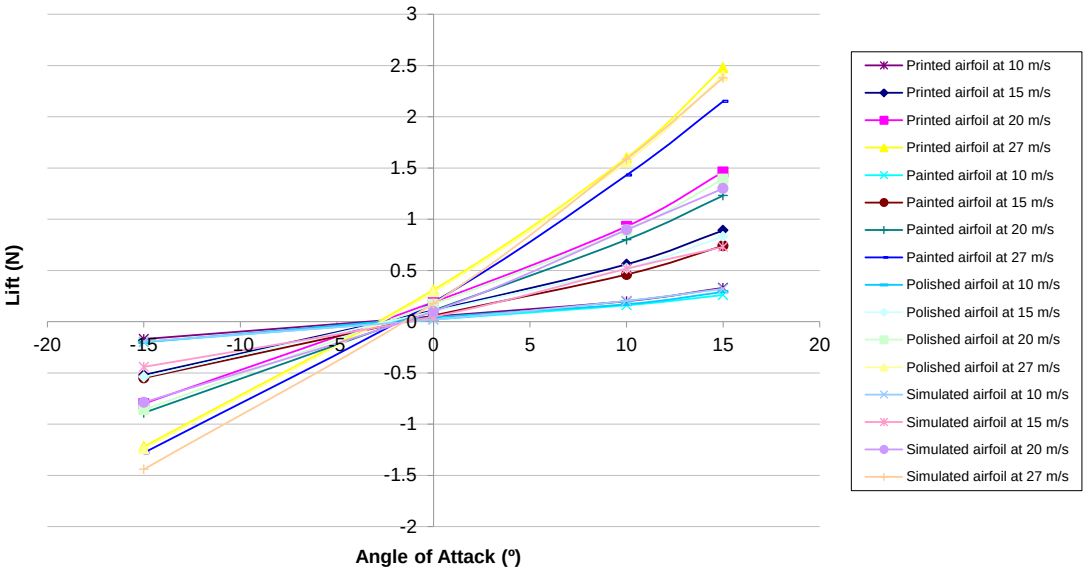

Figure 5 Plot of lift force Vs α from wind tunnel testing and simulation

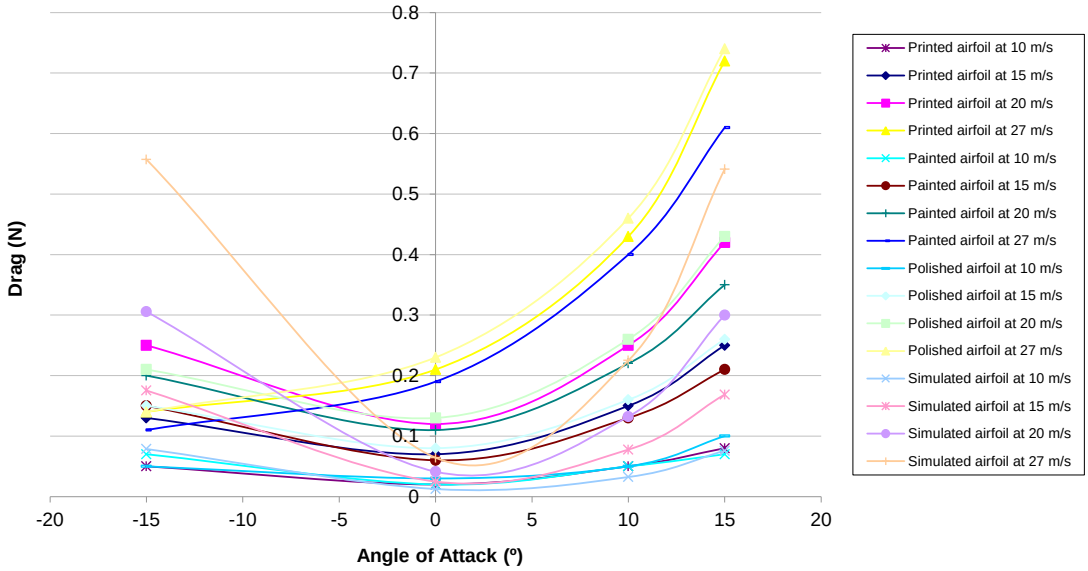

Figure 6 Plot of drag force Vs α from wind tunnel testing and simulation

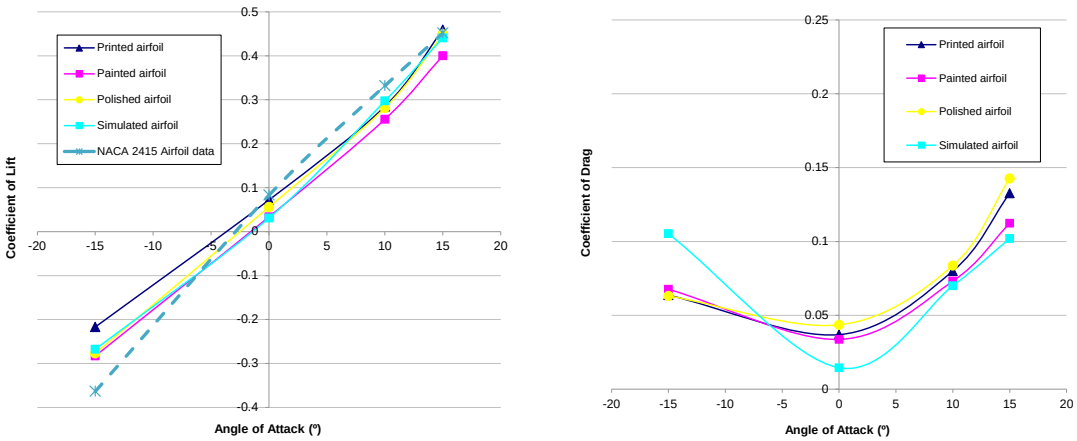

(a) (b)

Figure 7 (a) C_L Vs α plot from wind tunnel testing, simulation and NACA 2415 airfoil data and (b) C_D Vs α plot from wind tunnel testing and simulation

Table 4 Corresponding Finite Lift Slope (a)

Results	Finite Lift Slope (a)
Printed airfoil	0.0213
Painted airfoil	0.0222
Polished airfoil	0.0225
Simulated airfoil	0.0266
NACA 2415 airfoil data	0.0249

Figure 9 and 10 are showing the flow trajectories from the simulation at a velocity of 27 m/s and angles of attack of 0° and 15° respectively. At a high angle of attack, there was more strength of downwash forming wingtip vortices, which greatly increased induced drag. Flow separation was also noticeable toward the trailing edge on the upper surface of the airfoil. A larger area of boundary layer separation was presented, which increased total drag, therefore, declining of L/D ratio.

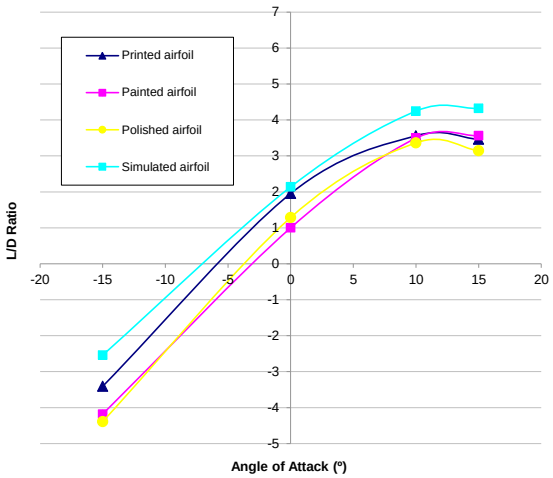

Figure 8 L/D ratio Vs α plot from wind tunnel testing and simulation

Table 5 Corresponding Reynolds Numbers

Air Velocity (m/s)	Reynolds Number
10	$8.2x10^4$
15	$1.2x10^5$
20	$1.6x10^5$
27	$2.2x10^5$

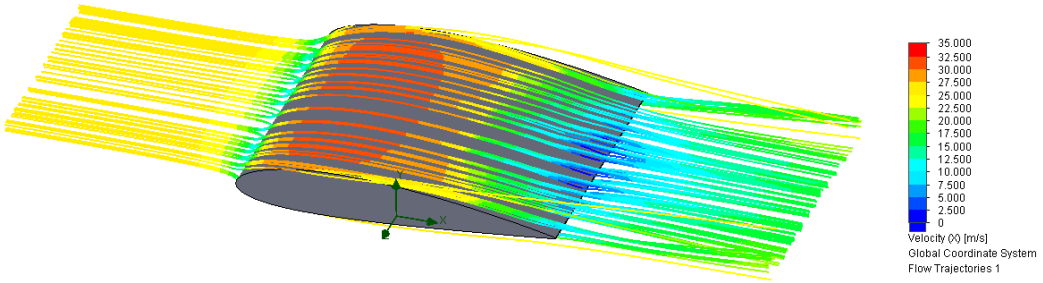

Figure 9 Simulation result at Re = $2.2x10^5$, α = 0º

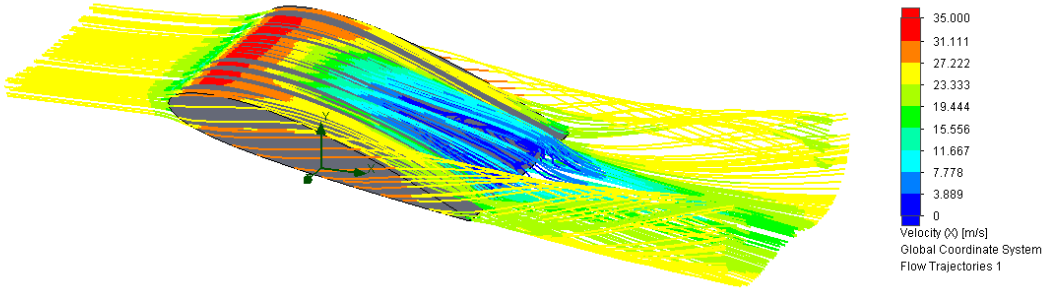

Figure 10 Simulation result at Re = $2.2x10^5$, α = 15º

5. Conclusion

3-dimensional NACA 2415 airfoil models were tested at 4 Reynolds numbers and three configuration models in a low-speed wind tunnel. All of them were printed by fused deposition modeling method. The first specimen represented a direct printed surface roughness without post-processing step. The second one was being primed and painted with acrylic lacquer with moderate surface finishing. Lastly, the other one was with high surface finishing with glossy polishing. Lift and drag force were obtained from the data acquisition system at different angles of attack and different air velocities. The results were then compared to the CFD model. Lift coefficients for all wind tunnel testing models matched well with the simulation; however, drag coefficients were inclusive below 10°. Different aerodynamic characteristics were observed between different roughness surface finishing specimens. The roughness of the airfoil surface could change the flow characteristics.

Fused deposition modeling (FDM) is a common manufacturing method for prototyping and scientific experimental usage, which is cost-effective and high geometry precision forming. Using different printed materials and parameter setups will result in a different level of surface roughness finishing. The aerodynamic objects, such as an airfoil shape specimen that has been manufactured from FDM printing

method, needs roughness validation before performing aerodynamic experimental testing. The effects of the surface roughness on aerodynamic objects can alter airfoil characteristics; thus, the improvement of the airfoil efficiency on different airfoil surface roughness areas can be further investigated.

6. Acknowledgements

The authors would like to extend our gratitude to Mr. Nopporn Pinitsap for the assistance providing wind tunnel apparatus setup at Fluid Mechanic Laboratory, College of Engineering, Rangsit University.

7. References

Abbott, I. H. & Doenhoff, A. E. (1959). *Theory of wing sections: Including a summary of airfoil data*. New York: Dover Publication, Inc.

Abdel-Rahman, A. A., & Chakroun, W. M. (1997). Suface Roughness Effects on Flow Over Aerofoils. *Wind Engineering*, *21*(3), 125-137.

Alsoufi, M., & Elsayed, A. (2017) How Surface Roughness Performance of Printed Parts Manufactured by Desktop FDM 3D Printer with PLA+ Influenced by Measuring Direction. *American Journal of Mechanical Engineering*, *5*(5), 211-222.

Anderson, J. D. (2012). *Introduction to Flight*. New York: McGraw-Hill.

Ghods, M. (2001). Theory of Wings and Wind Tunnel Testing of A NACA 2415 Airfoil. The University of British Columbia.

Harun, Z., Abbas, A., Dheyaa, M., & Ghazali, M. (2016). Ordered Roughness Effects on NACA 0026 Airfoil. *AEROTECH VI – Innovation in Aerospace Engineering and Technology*, *152*(012005), 1-9.

Jain, R., Jain, S., & Bajpai, L. (2016). Investigation on 3-D Wing Commercial Aeroplane with Aerofoil NACA 2415 Using CFD Fluent. *International Research Journal of Engineering & Technology*, *3*(6), 243-249.

Krolczyk, G., Raos, P., & Legutko, S. (2014). Experimental Analysis of Surface Roughness and Surface Texture of Machined and Fused Deposition Modelled Parts. *Tehnički Vjesnik*, 21(1), 217-221.

Kumar, V., Tomar, V., Kumar, N., & Jain, S. (2015). Flow Simulation and Theoretical Investigation on Aerodynamics of NACA-2415 Aerofoil at Low Reynolds Number. *SAE Technical Paper*, 2015-01-2576, 1-8.

Olasek, K., & Wiklak, P. (2014). Application of 3D printing technology in aerodynamic study. *Journal of Physics: Conference Series*, *530* (012009), 1-7.

Parashar, H. (2015). Calculation of Aerodynamic Characteristics of NACA 2415, 23012, 23015 Airfoils Using Computational Fluid Dynamics (CFD). *International Journal of Science, Engineering and Technology Research*, *4*(3), 610-614.

Rodríguez, I., Lehmkuhl, O., Piomelli, U., Chiva, J., Borrell, R., & Oliva, A. (2016). Numerical Simulation of Roughness effects on the Flow Past Circular Cylinder. *Journal of Physics: 7th European Thermal-Science Conference*, *745*(032043), 1-8.

Selig, M., Lyon, C., Giguere, P., Ninham, C., & Guglielmo, J. (1996) *Summary of Low-Speed Airfoil Data: Volume 2*. Virginia: SoarTech Publications.

Sogukpinar, H., & Bozkurt, I. (2015). Calculation of Aerodynamic Performance Characteristics of Airplane Wing and Comparing with the Experimental Measurement. *International Journal of Engineering Technologies*, *1*(2), 83-87.

Srivastava, A., Tiwari, V., & Singh, K.R. (2017). Numerical Simulation of NACA 2415 Airfoil: At Different Low Reynolds Numbers and Angle of Attack. *International Journal of Research in Mechanical Engineering & Technology*, *7*(2), 33-37.

Smith, H.C. (1992). *The Illustrated Guide to Aerodynamics*. New York: McGraw-Hill.

Velázques, L., & Nožička, J. (2013). Computational Simulation of the Flow Past an Airfoil for an Unmanned Aerial Vehicle. *Systemics, Cybernetics and Informatics*, *11*(6), 40-46.

Velázques, L., & Nožička, J. (2014). Computational Simulation of the 2415-3S Airfoil Aerodynamic Performance. *Systemics, Cybernetics and Informatics*, *12*(1), 46-51.

Velázques, L., Nožička, J., & Vavřín, J. (2010). Experimental Measurement of the Aerodynamic characteristics of Two-Dimensional Airfoils for an Unmanned Aerial Vehicle. *Proceedings of Experimental Fluid Dynamics, EPJ Web of Conferences*, *25*(02027), 1-11.

White, E. B., Kutz, D., Freels, J., Hidore, J. P., Grife, R., Sun, Y., & Chao, D. (2011). Leading-Edge Roughness Effects on 633-418 Airfoil Performance. *49th AIAA Aerospace Sciences Meeting*.

Zhou, Y., & Wang, Z. J. (2012). Effects of Surface Roughness on Separated and Transitional Flows over a Wing. *AIAA Journal*, *50*(3), 593-609.